Chin. J. Astron. Astrophys. Vol. 7 (2007), No. 3, 380–388
(*http://www.chjaa.org*)

Chinese Journal of
Astronomy and
Astrophysics

A Possible 456-Day Optical Period of OQ 530 *

Yi Liu, Juan Li and Jun-Hui Fan

Center for Astrophysics, Guangzhou University, Guangzhou 510006; *jhfan_cn@yahoo.com.cn*

Received 2006 September 12; accepted 2007 April 27

Abstract The post-1994 observations of the blazar OQ 530 in optical $BVRI$ bands, and radio observations at 22 GHz and 37 GHz were collected. The date compensated discrete Fourier transform (DCDFT) and CLEANest methods were used to search for possible periodicities. Two possible periods of 456 ± 100 days and 258 ± 29 days were found in the optical bands. The existence of possible correlations between the optical and radio emissions was investigated by means of discrete correlation function (DCF) analysis, and no significant correlation was found. Some possible mechanisms for the periodic variability are discussed.

Key words: galaxies: active — BL Lacertae objects: general — BL Lacertae objects: individual: OQ 530

1 INTRODUCTION

Blazars are a subclass of active galactic nuclei (AGNs) with some extreme observational properties, including rapid and large amplitude variabilities of flux, high optical linear polarizations, and superluminal motions. They have been main monitoring targets for a long time.

The variabilities are an important feature of blazars. The observed variabilities of many sources show obvious periodicity. The periodicity of variability can inform us on the structure of its central source structure and the energy production processes therein. Based on the observed periodicity of minimum light in PKS 1510–089, Xie et al. (2002) proposed a binary black hole (BBH) model, with an orbital period of 336 days (Wu et al. 2005; Li et al. 2006). Another well-studied example is OJ 287. Its historical light curve shows a precise periodicity of 11.86 years, and Sillanpää et al. (1988) proposed a BBH model to explain it. Kidger et al. (1992) confirmed the 11-year periodicity with the Jurkevich method (Jurkevich 1971) and predicted the time of next outburst, and then found the next burst occurred almost exactly at the predicted time. Again, Rieger & Mannheim (2000) claimed that Mkn 501 has a periodicity of 23 days in X and γ ray bands. Liu et al. (1995) analyzed the historical light curve of ON 231 and found a period of 13.65 years. For BL Lac 2200+400, a 14 year period was found in the B band light curve (Fan et al. 1998). Periodicity analysis was performed on the optical data of some sources by Fan et al. (2002) and on the radio data by Fan et al. (2007).

OQ 530 (B1418+546, $z = 0.152$) is a very active BL Lac object. It was optically identified in 1977 (Kuehr 1977), as the counterpart of an extragalactic source included in the NRAO-Bonn radio survey at 5 GHz. It was classified as a BL Lac by Miller (1978), because of its stellar aspect and the faintness of its optical spectral features. Its long term optical variability is characterized by a decreasing trend in the mean luminosity. Carini et al. (1990) analyzed the optical data and failed to find any possible periodicity. That may be caused by poor sampling in the older data. Fan et al. (2002) compiled and analyzed its historical light curve, but they also failed to find any period.

Correlations between the variations in different frequency regions have been found in many sources. Hanski et al. (2002) compared the radio light curves with the optical ones of 20 sources, the radio curves

* Supported by the National Natural Science Foundation of China.

were from the Metsähovi monitoring program, and the optical curves were from the literature. Using the Discrete Correlated Function (DCF, hereafter) (Edelson & Krolik 1988) analysis, seven sources were found to show clear correlations, and six others to show possible correlations between the optical and radio events, with time lags ranging from zero to several hundred days. Their results are consistent with those of Tornikoski et al. (1994) and Clements et al. (1995), who also analyzed a large sample of AGNs. OQ 530 was included in their sample, but no significant correlations were found in this object.

In this paper, we collected the new available post-1994 optical data, together with the radio band emission data from available literature, and searched for possible periodicity by using the periodicity analysis method that we adopted in our previous works (Fan et al. 2006, 2007). We investigated possible correlated variations using the DCF method. This paper is arranged as follows. In Section 2, we give the optical and radio light curves. The date compensated discrete Fourier transform (DCDFT) (Ferraz-Mello 1981; Foster 1995) and CLEANest (Foster 1995; Liu et al. 2006) methods are used to search for the possible periodicities. In Section 3 we analyze the optical data and the radio data from the Metsähovi monitoring program to investigate the existence of possible correlations between them by DCF analysis. We discuss the results and give conclusions in Section 4.

2 LIGHT CURVES AND PERIODICITY ANALYSIS

2.1 Optical Light Curves

The monitored optical light curves are shown in Figure 1. We collected the data from Massaro et al. (2004), the monitoring was from 1994 June to 2001 July. All their photometric monitoring of OQ 530 in the four bands B, V(Johnson) and R, I (Cousins) are presented here, in the panels from bottom up.

Many large-amplitude outbursts can be seen in Figure 1. The minimum and maximum magnitudes observed were, respectively, 15.21 ± 0.05 (JD=2450262) and 16.95 ± 0.07 (JD=2450863) in the B band, 14.44 ± 0.05 (JD=2450994) and 16.15 ± 0.03 (JD=2450860) in the V band, 14.33 ± 0.02 (JD=2450263) and 15.80 ± 0.12 (JD=2451299) in the R band, and 13.72 ± 0.03 (JD=2452052) and 15.10 ± 0.09 (JD=2449909) in the I band. There are 117 data points in the B band, 169 in the V band, 305 in the R band and 249 in the I band. Since there are more data points in the R and I bands, our analysis is mainly based on these two bands.

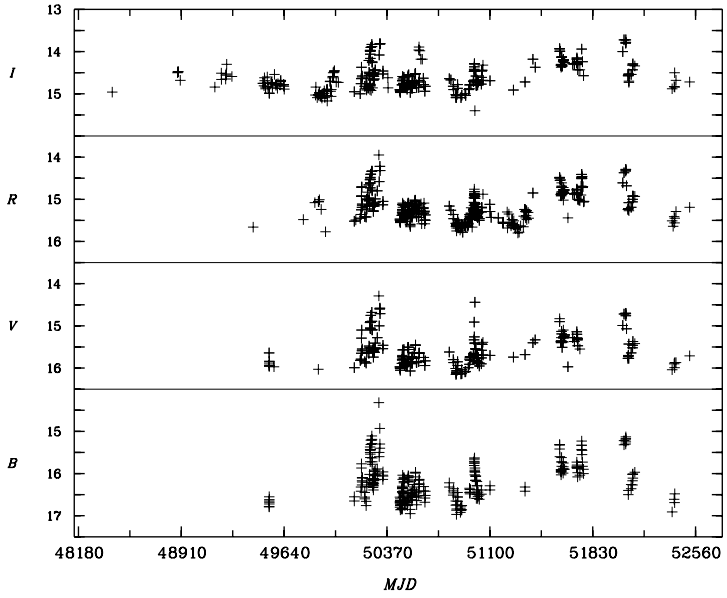

Fig. 1 Light curves of OQ 530. From bottom up, the panels show the B, V, R and I light curves. The data were collected from Massaro et al. (2004).

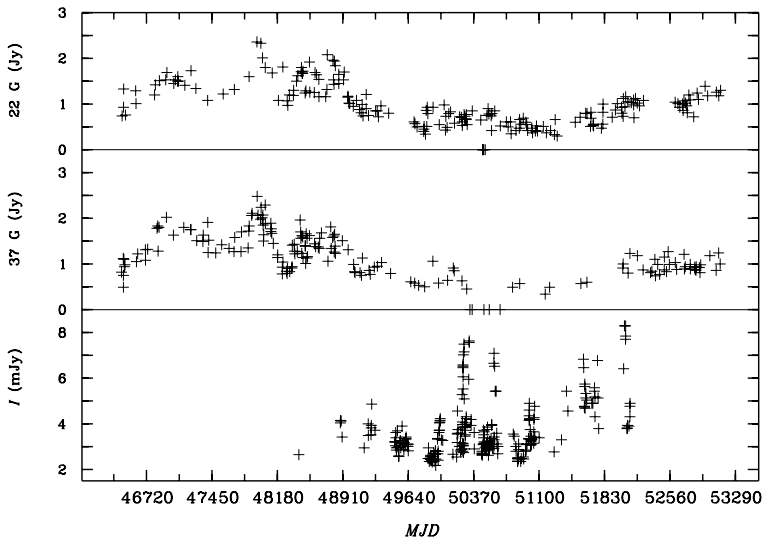

Fig. 2 Radio and optical light curves of OQ 530. From bottom up, the panels show the I band light curve, the radio 37 GHz light curve and the 22 GHz light curve.

OQ 530 has been monitored in radio bands by the Metsähovi Radio Observatory in Finland since 1985. Figure 2 shows long term radio light curves of OQ 530 at 37 GHz and 22 GHz, collected from Teräsranta et al. (1992, 1998, 2004, 2005). We also analyzed these radio data.

2.2 Periodicity Analysis: Method

We performed a power spectral (Fourier) analysis on these data. To deal with data that are unevenly spaced in time, attempts have been made including the *modified periodogram* (Scargle 1982; Horne & Baliunas 1986), and a better technique is the DCDFT (Ferraz-Mello 1981; Foster 1995). The DCDFT method is a more powerful method than the *modified periodogram* (Foster 1995); it is based on a least-square regression on three trial functions, $\sin(\omega t)$, $\cos(\omega t)$ and constant, $\omega = 2\pi f$, f is the frequency. We applied DCDFT to the R, I and radio light curves (see Fan et al. 2006; Foster 1995 for a detail).

We adopted another tool, *False Alarm Probability* (FAP; Horne & Baliunas 1986), to give a quantitative criterion for the detection of a periodic signal derived by DCDFT. Horne & Baliunas (1986) introduced the FAP to deal with the modified periodogram, which represents the probability that the highest peak of frequency produced from a white noise is less than a power value z. In fact, the FAP can deal with all kinds of Fourier analysis method if the variations (mainly) consist of randomly distributed noise. In Figures 3, 4, 6 and 7 we notice that the noise is almost randomly distributed. Its various steps are described in Fan et al. (2006).

Irregular spacing in unevenly sampled time series introduces myriad complications into the Fourier transform, even the DCDFT. It can alter the peak frequency (slightly) and amplitude (greatly), and can even introduce extremely large false peaks.

In this paper we use Foster's (1995) CLEANest analysis to clean out false periodicity and remove the false peaks. The strongest single peak and corresponding false components are subtracted first from the original spectrum, then the residual spectrum is scanned to determine whether the strongest remaining peak is statistically significant. If so, then the original data are analyzed to find the pair of frequencies which best models the data, these two peaks and corresponding false components are subtracted, and the residual spectrum is scanned. The process is repeated until all statistically significant frequencies are included, producing the CLEANest spectrum. We obtained the CLEANest spectrum by iterative process (Liu et al. 2006). We assume that there are five independent frequency components in the observational data. The CLEANest spectrum is shown in Figures 3, 4, 6 and 7 and the numerical results are listed in Tables 1 and 2.

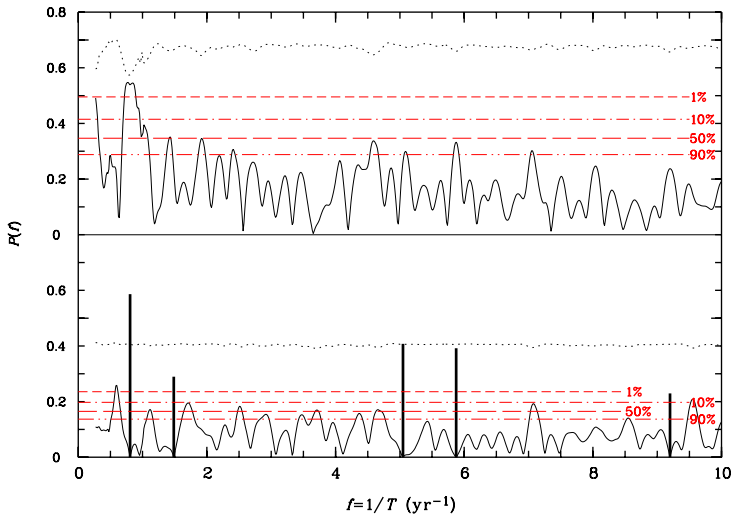

Fig. 3 Fourier analysis and CLEANest results for the R band light curve. The upper panel shows the Fourier analysis result of the adopted light curve and the lower panel is the corresponding CLEANest spectrum. The dotted curve marks the square deviation at different frequencies. In the CLEANest spectrum five CLEANest frequency components (spikes) and the residual spectrum are shown. Various significance levels are marked.

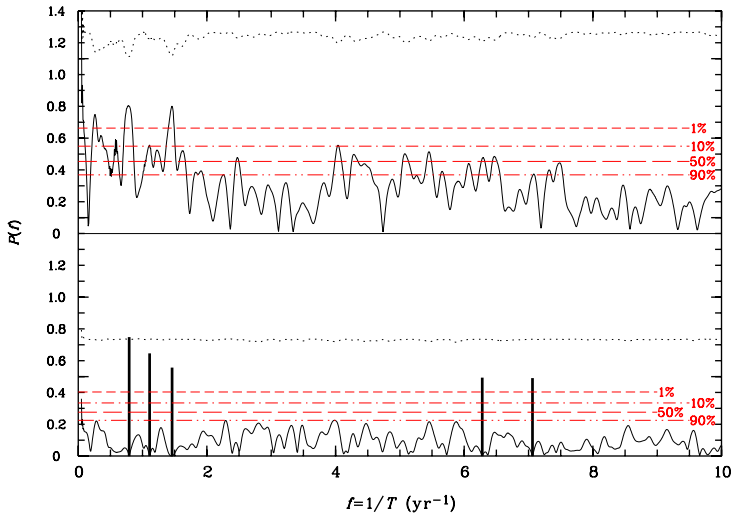

Fig. 4 Same as Figure 3, except for the I light curve.

2.3 Periodicity Analysis Results of the R and I Data

We list our results of periodicity analysis derived with DCDFT and CLEANest in Table 1. Four possible periods in the R data are obtained. In Figure 3, the upper panel shows the DCDFT result of the whole R data, and the lower panel shows that of CLEANest. In Figure 3 the strongest signal is located at $f_1 = 0.806 \pm 0.176\,\mathrm{yr}^{-1}$ corresponding to $P_1 = 452 \pm 99\,\mathrm{d}$, and the next strong peak is located at $f_2 = 1.485 \pm 0.176\,\mathrm{yr}^{-1}$, corresponding to $P_2 = 246 \pm 29\,\mathrm{d}$. In the I band, five possible periods are derived by DCDFT and CLEANest. See Figure 4. The upper panel presents the DCDFT result, and the lower panel the corresponding CLEANest result. The strongest signal is located at $f_1 = 0.792 \pm 0.171\,\mathrm{yr}^{-1}$,

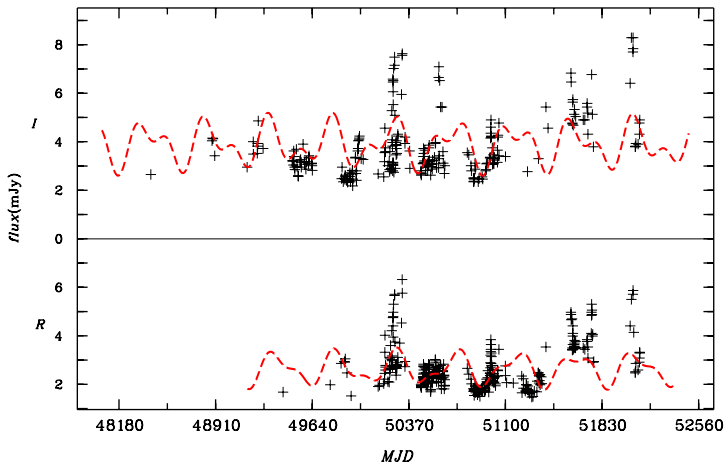

Fig. 5 R and I band light curves of OQ 530. The dashed curves are the theoretical results obtained by using two selected CLEANest components.

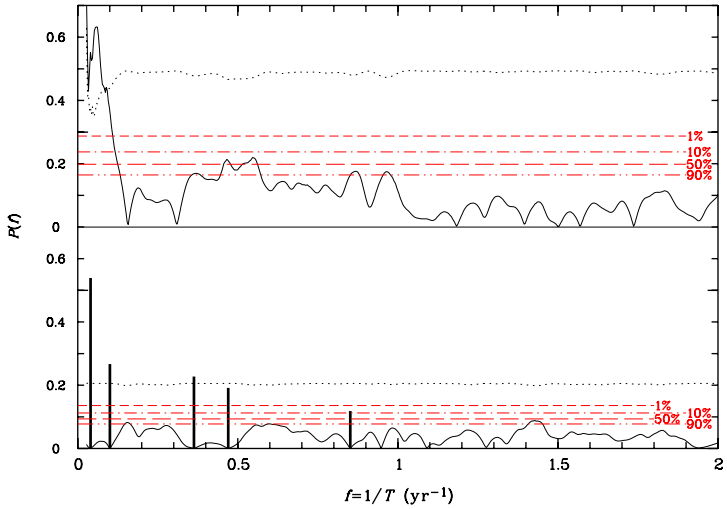

Fig. 6 Same as Figure 3, except for the 37 GHz radio curve.

corresponding to $P_1 = 461 \pm 100$ d. The third strongest signal is located at $f_2 = 1.460 \pm 0.171\,\mathrm{yr}^{-1}$, corresponding to $P_2 = 250 \pm 29$ d.

Combining the R and I band data results, we obtain, in the optical band of OQ 530, the periodicities, $P_1 = 456 \pm 100$ d = 1.25 ± 0.27 yr and $P_2 = 248 \pm 29$ d. We compare R and I light curves with the theoretical results obtained by using some strongest CLEANest components in Figure 5.

2.4 Results of Periodicity Analysis of the Radio Data

DCDFT and CLEANest were applied to the radio data. There are 143 data points in 22 GHz and 70 data points in 37 GHz. The corresponding periodicity analysis results are presented in Table 2.

In the 37 GHz data, five CLEANest components are obtained. The results of DCDFT and CLEANest are shown in Figure 5. The strongest one is located at $P = 9109$ d = 25 yr, which is longer than the observation

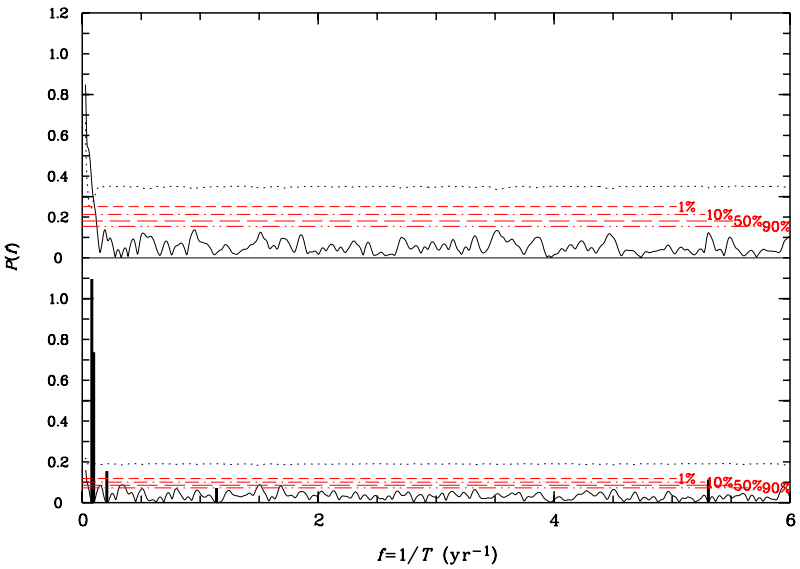

Fig. 7 Same as Figure 3, except for the RADIO 22 GHz light curve.

Table 1 The CLEANest Results Derived from the Optical Data

R band				I band			
Period (d)	Amplitude (mJy Hz^{-1})	Phase (π rad)	FAP	Period (d)	Amplitude (mJy Hz^{-1})	Phase (π rad)	FAP
452 ± 99	0.587 ± 0.170	-0.017 ± 0.274	$\ll 0.01$	461 ± 100	0.749 ± 0.292	-0.036 ± 0.344	$\ll 0.01$
				329 ± 51	0.646 ± 0.292	-0.449 ± 0.374	$\ll 0.01$
246 ± 29	0.290 ± 0.170	0.241 ± 0.829	$\ll 0.01$	250 ± 29	0.557 ± 0.292	0.536 ± 0.461	$\ll 0.01$
72 ± 2.5	0.408 ± 0.170	-0.163 ± 0.160	$\ll 0.01$				
62 ± 1.9	0.392 ± 0.170	0.321 ± 0.598	$\ll 0.01$	58 ± 1.6	0.494 ± 0.292	0.993 ± 0.578	$\ll 0.01$
				52 ± 1.3	0.491 ± 0.292	-0.399 ± 0.380	$\ll 0.01$

Table 2 The CLEANest Results Derived from the Radio Data

37 GHz				22 GHz			
Period (d)	Amplitude (mJy Hz^{-1})	Phase (π rad)	FAP	Period (d)	Amplitude (mJy Hz^{-1})	Phase (π rad)	FAP
9109 ± 16139	0.539 ± 0.098	-0.833 ± 0.182	$\ll 0.01$				
3626 ± 2558	0.267 ± 0.098	0.262 ± 0.367	$\ll 0.01$	4451 ± 4071	1.096 ± 0.090	0.123 ± 0.082	$\ll 0.01$
				3767 ± 2916	0.737 ± 0.090	-0.870 ± 0.122	$\ll 0.01$
				1750 ± 630	0.156 ± 0.090	-0.217 ± 0.578	$\ll 0.01$
1006 ± 197	0.228 ± 0.098	-0.934 ± 0.430	$\ll 0.01$				
776 ± 117	0.192 ± 0.098	-0.575 ± 0.511	$\ll 0.01$				
429 ± 36	0.119 ± 0.098	0.757 ± 0.824	0.09				
				69 ± 1	0.114 ± 0.090	0.948 ± 0.791	0.05

time coverage ($\sim$ 19 yr) and so can not be a physically meaningful period. The second one is located at $P = 3626 \pm 2558$ d, with a amplitude 0.267 ± 0.098 Jy and a phase $0.262 \pm 0.367\pi$ rad.

For the 22 GHz data, four CLEANest components are listed in Table 2, and the results of DCDFT and CLEANest are displayed in Figure 7. The strongest one is located at $P = 4451 \pm 4071$ d, with an amplitude 1.096 ± 0.090 Jy and a phase $0.123 \pm 0.082\pi$ rad.

3 RADIO AND OPTICAL CORRELATION

In Figure 2, the long-term radio light curves of OQ 530 in 37 GHz and 22 GHz are shown (the flux in units of Jy). In order to make comparison, the I band optical light curve (in units of mJy) collected from Massaro et al. (2004), is also shown in Figure 2. According to Mead et al. (1990), zero magnitude in I band corresponds to $S_0 = 2.55$ kJy in flux. The magnitudes were then converted to flux according to

$$S = S_0 \times 10^{-\frac{M}{2.5}}. \tag{1}$$

We can see from Figure 2 that the optical variations seem to be much more frequent and obvious than the radio ones, and with much larger amplitudes between 1994 and 2001. There are only minor enhancements in the radio flux when optical outbursts are seen, which suggests that the mechanism responsible for optical outburst only partially affects the radio emission.

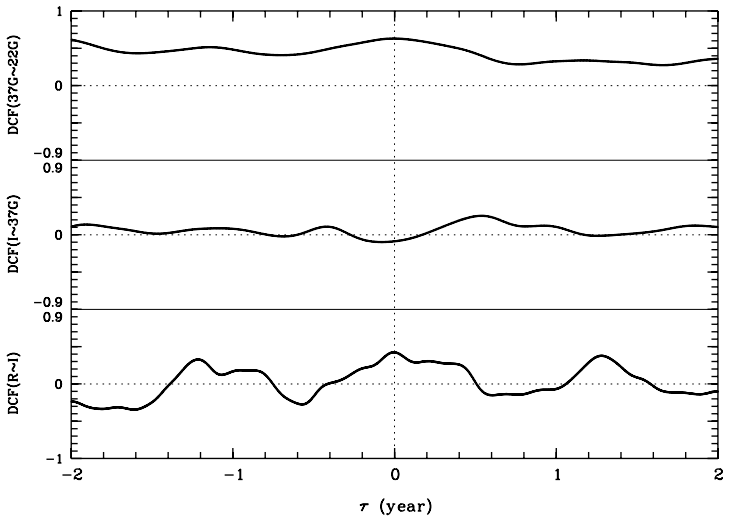

Fig. 8 DCF results of the optical and radio data of OQ 530. The bottom panel is for the DCF between the R and I data, the middle one, between the I and 37 GHz radio data, and the top one, between the radio 37 GHz data and the 22 GHz data (DCF bin size: 60 days).

3.1 DCF Method

The DCF was used to analyze the data shown in Figure 2 to investigate the optical-radio correlation: it is a method specifically designed for unevenly sampled datasets (Edelson & Krolik 1988); it also allows an estimation of the accuracy of its results. Given two datasets, a_i and b_j, one has to combine all pairs to calculate the unbinned discrete correlations:

$$\mathrm{UDCF}_{ij} = \frac{(a_i - \bar{a})(b_j - \bar{b})}{\sigma_a \sigma_b}, \tag{2}$$

where $\bar{a}$, $\bar{b}$ are the average values of the two datasets, and σ_a, σ_b are the standard deviations. The DCF is obtained by binning the UDCF_{ij} in time for each time lag τ:

$$\mathrm{DCF}(\tau) = \frac{1}{M} \sum \mathrm{UDCF}_{ij}, \tag{3}$$

where M is the number of pairs (a_i, b_j) with time lag $\triangle_{ij} = t_j - t_i$ inside the τ bin. Spurious correlations can arise of the order of $\pm M^{-\frac{1}{2}}$. The standard error for each bin is:

$$\sigma_{\mathrm{DCF}}(\tau) = \frac{1}{M-1} \{ \sum [\mathrm{UDCF}_{ij} - \mathrm{DCF}(\tau)]^2 \}^{\frac{1}{2}}. \tag{4}$$

A positive peak of the DCF means correlation, which is the stronger as the value of the peak approaches and exceeds one. A negative peak means anticorrelation. Moreover, the width of the peak must be comparable to those of the autocorrelation functions, obtained by applying the DCF to each dataset coupled with itself.

A preliminary binning of data in time before calculating the DCF usually leads to better results by smoothing out fluctuations. An increase of the data binning interval implies an increase of spurious correlations, while an increase of the DCF bin size has the opposite effect. Also the choice of the DCF bin size is a delicate point, involving a balance between resolution and noise.

3.2 Results by DCF

The upper, middle and lower panel of Figure 8 presents the results of DCF cross-correlation between (1) 37 GHz and 22 GHz, (2) I and 37 GHz, and (3) R and I. We can see from Figure 8 that correlations between 37 GHz and 22 GHz, and between R and I are strong, while that between I and 37 GHz is very weak. This result is consistent with results of Clements et al. (1995).

4 DISCUSSION AND CONCLUSIONS

Periodicity analysis method is important when searching for periodicity in uneven sampled time series. The Jurkevich method is simple but it cannot avoid harmonic components, and it does not give statistical significance of the claimed period. In contrast, the DCDFT and CLEANest methods do. Hence these are used in this paper to search for possible periodicity in the optical data, and one on a timescale of 456 day was found. This periodicity was not found in some previous works, possibly because of the data were sparse, nor in our previous work did we find any clear long-term period in this source (Fan et al. 2002). This period is not very clear in the radio bands, however.

Correlation between the optical and radio emissions was investigated using the DCF method, and no obvious correlation was found, consistent with the previous results of Tornikoski et al. (1994) and Clements et al. (1995). This result is also consistent with the periodicity analysis result above.

As mentioned in the introduction, periodic variability has been found in many sources and many models have been proposed to explain this phenomenon (Fan 2005): the binary black hole model, helical jet model, slim disk model, and change of accretion rate. The binary black hole model offers a promising explanation, and has been applied to many sources, including OJ 287, PKS 1510–089, Mkn 501, 3C 120 (Caproni & Abraham 2004a) and 3C 345 (Caproni & Abraham2004b). However, high precision VLBI observation is needed to confirm the predictions. The helical jet model may be a possible explanation for the periodic variability in OQ 530. In this model, as suggested by Villata & Raiteri (1999), variability in blazars could be due to changes in the orientation of the emitting jet, probably caused by the orbital motion of the parent black hole in a binary black hole system (BBHS), and hence due to a change of the relativistic beaming factor, where the emission of the jet is produced by relativistic electrons that are responsible for producing both the low-energy (from radio to X-rays) synchrotron radiation and the high-energy (up to γ-rays) one through inverse-Compton (IC) scattering of the same synchrotron photons (synchrotron-self- Compton process, SSC). This model has been applied to many sources to explain the variability, including Mkn 501, AO 0235+16 (Raiteri et al. 2001), ON 231 (Sobrito et al. 2001) and others. VLBI observations of OQ 530 (Cassaro et al. 2002) showed that the jets on parsec and kiloparsec scales are misaligned by about 150 degree, which is also a support for the binary black hole model. The period of 465 day in OQ 530 may possibly be caused by a helical jet.

In this paper, both DCDFT and CLEANest methods are used to search for possible periodicities in OQ 530 in the optical bands. A possible period of 456 days was found. Correlation between the optical and radio emission was investigated and found to be very weak.

Acknowledgements The authors wish to thank Dr. Wang H.-G., Chen J.-L., Zhou J.-L. and Yuan Y.-H for some useful discussions. This work was supported by the National Science Fund for Distinguished Young Scholars (10125313), the National Natural Science Foundation of China (Grants 10573005 and 10633010). We also thank the financial support from the Guangzhou Education Bureau and Guangzhou Science and Technology Bureau. This research has made use of data from the University of Michigan Radio Astronomy Observatory which has been supported by the University of Michigan and the National Science Foundation. We thank the referee for the useful comments and suggestions.

References

Caproni A., Abraham Z., 2004, MNRAS, 349, 1218
Caproni A., Abraham Z., 2004, ApJ, 602, 625
Carini M. T., Miller H. R., Goodrich B. D., 1990, AJ, 100, 347
Cassaro P., Stanghellini C., Dallacasa D. et al., 2002, A&A, 381, 378
Clements S. D., Smith A. G., Aller H. D. et al., 1995, AJ, 110, 529
Edelson R. A., Krolik J. H., 1988, ApJ, 333, 646
Fan J. H., 2005, Chin. J. Astron. Astrophys. (ChJAA), 5S, 213
Fan J. H., Lin R. G., Xie G. Z. et al., 2002, A&A, 381, 1
Fan J. H., Liu Y., Yuan Y. H. et al., 2007, A&A, 462, 547
Fan J. H., Tao J., Qian B. C. et al., 2006, PASJ, 58, 797
Fan J. H., Xie G. Z., Pecontal E. et al., 1998, ApJ, 507, 173
Ferraz-Mello S., 1981, AJ, 86, 619
Foster G., 1995, AJ, 109, 1889
Hanski M. T., Takalo L. O., Valtaoja E., 2002, A&A, 394, 17
Horne J., Baliunas S., 1986, ApJ, 302, 757
Jurkevich I., 1971, Ap&SS, 13, 154
Kidger M., Takalo L., Sillanpää A., 1992, A&A, 264, 32
Kuehr H., 1977, A&AS, 29, 139
Li J., Fan J. H, Yuan Y. H., 2007, Chin. Phy., 16, 876
Liu F. K., Xie G. Z., Bai J. M., 1995, A&A, 295, 1
Liu Y., Fan J. H., Wang H. G. et al., 2006, Chin. J. Astron. Astrophys. (ChJAA), 6S2, 357
Massaro E., Mantovani F., Fanti R. et al., 2004, VizieR Online Data Catalog, 342, 30935
Mead A. R. G., Ballard K. R., Brand P. W. J. L. et al., 1990, A&AS, 83, 183
Miller H. R., 1978, ApJ, 223, 67
Raiteri C. M., Villata M., Aller H. D. et al., 2001, A&A, 377, 396
Rieger F. M., Mannheim K., 2000, A&A, 359, 948
Scargle J., 1982, ApJ, 263, 835
Sillanpää A., Haarala S., Valtonen M. J. et al., 1988, ApJ, 325, 628
Sobrito G., Raiteri C. M., Villata M. et al., 2001, Memorie della Societa Astronomica Italiana, 72, 149
Teräsranta H., Achren J., Hanski M. et al., 2004, A&A, 427, 769
Teräsranta H., Tornikoski M., Mujunen A. et al., 1998, A&AS, 132, 305
Teräsranta H., Tornikoski M., Valtaoja E. et al., 1992, A&AS, 94, 121
Teräsranta H., Wiren S., Koivisto P. et al., 2005, A&A, 440, 409
Tornikoski M., Valtaoja E., Terasranta H. et al., 1994, A&A, 289, 673
Wu J., Zhou X., Peng B. et al., 2005, MNRAS, 361, 155
Villata M., Raiteri C. M., 1999, A&A, 347, 30
Xie G. Z., Liang E. W., Zhou S. B. et al., 2002, MNRAS, 334, 459